European Review for Medical and Pharmacological Sciences 2020; 24: 4793-4802

Autophagy related 4B, upregulated by HIF-1α, attenuates the sensitivity to cisplatin in nasopharyngeal carcinoma cells

J. HUANG, H.-B. LI, S. YU, F. YUAN, Z.-P. LOU

Department of Otolaryngology, Zhuji Affiliated Hospital of Shaoxing University, Zhuji City, Zhejiang Province, China

Abstract. – OBJECTIVE: Increasing evidence has shown that autophagy related proteins and hypoxia-inducible factor-1α (HIF-1α) are both involved in the malignant progress of nasopharyngeal carcinoma (NPC), and HIF-1α plays an emerging role in the chemosensitivity of NPC cells. However, it is still unknown whether autophagy related proteins are associated with HIF-1α in regulating the chemosensitivity of NPC cells.

MATERIALS AND METHODS: Quantitative Real-time PCR (qPCR) was applied to determine mRNA levels of HIF-1α and the autophagy related proteins, such as ATG3, ATG4B, ATG5, Beclin1, ATG7, ATG10, ATG12 and ATG16L1. Western blot was applied to determine protein levels of HIF-1α, ATG4B and cleaved Caspase-3. Cell viability and death were investigated by cell counting kit-8 and trypan blue exclusion assay. In addition, Caspase-3 activity was detected to reflect apoptosis. Furthermore, Luciferase reporter assay was applied to explore the mechanism by which HIF-1α transcriptionally upregulated ATG4B expression.

RESULTS: Our study reveals that HIF-1α increased ATG4B expression in NPC cells, and in turn upregulated the cisplatin (DDP)-induced protective autophagy, resulting in enhanced killing effect of DDP to NPC cells. In mechanism, reporter assay showed that HIF-1α upregulated ATG4B expression by activating its gene promoter region. The binding site (-225 to -216) was required for HIF-1α-induced increase of ATG4B gene promoter activity.

CONCLUSIONS: These results indicate that HIF-1α elevates ATG4B via promoting its transcription, which alleviates the sensitivity of DDP in NPC cells through enhancing protective autophagy, suggesting that ATG4B, upregulated by HIF-1α, may be a novel target for DDP sensitization in the treatment of NPC in clinic.

Key Words:
HIF-1α, ATG4B, NPC, DDP, Autophagy, Apoptosis.

Abbreviations

HIF-1α = Hypoxia-inducible factor-1α; ATG4B = Autophagy related 4B; NPC = Nasopharyngeal carcinoma; DDP = Cisplatin; CCK-8 = Cell Counting Kit-8; DMEM = Dulbecco's Modified Eagle Medium; qPCR = Quantitative real-time polymerase chain reaction; RIPA = Radioimmunoprecipitation assay; GAPDH = Glyceraldehyde 3-phosphate dehydrogenase; PBS = Phosphate buffered saline; Act D = Actinomycin D.

Introduction

Nasopharyngeal carcinoma (NPC) is one of the most common malignant tumors around the world[1]. It is also one of the most common malignancies in China, with the highest incidence among otorhinolaryngologic cancers[2]. Except for surgical resection and radiotherapy, chemotherapy is one of the main strategies for NPC treatment[3,4]. While the chemotherapeutic efficacy of NPC is still unsatisfactory[3,4]. Some reports[5-7] have shown that chemotherapeutic reagents can activate multiple survival mechanisms in the treatment of NPC, which can avoid cell death and lead to chemoresistance. Therefore, it is of great significance to explore the potential survival mechanisms of NPC for improving the chemotherapeutic efficacy of NPC.

Autophagy related proteins are a series of proteins that play an important role in autophagy, which can protect cancer cells from death and ultimately reduce the efficacy for tumor treatment[8-11]. It has been reported that autophagy related proteins are involved in the malignant progress of NPC[12-15]. The activation of the Beclin1/Bcl-2 signaling pathway induced by Angiotensin-(1-7) enhances autophagy level and in turn inhibits tumor growth in NPC xenografts[14]. Inhibition of Beclin1 and ATG5-dependent autophagy promotes nasopharyngeal carcinoma cell

Corresponding Author: Zhiping Lou, MD; e-mail: jiajiaamao@163.com

invasion and metastasis[12]. Autophagy adaptor protein SQSTM1 mediated epithelial to mesenchymal transition (EMT) promotes NPC metastasis. In NPC patients, high SQSTM1 expression is associated with increased risk of distant metastasis[13]. The metastasis of tumor is one of the most important causes of treatment failure in NPC[13]. These studies suggest that targeting autophagy related proteins may help to improve the efficacy for NPC treatment.

Hypoxia-inducible factor-1α (HIF-1α) plays a key role in cell survival under hypoxia condition in mammalian cells[16,17]. Previous studies have reported that HIF-1α promotes malignant transformation by binding to its target gene and exerting its transcriptional activity[18]. HIF-1α transcriptionally regulates many key aspects of tumor development and progression by promoting a more aggressive tumor phenotype, including the increase of proliferation and invasiveness as well as neoangiogenesis[19,20]. As to NPC, it has been reported that hypoxia is associated with aggressive phenotypes and poor outcomes, and HIF-1α depletion in hypoxic NPC cells leads to significantly reduced cell migration and invasion[21]. Additionally, overexpression of HIF-1α restores the long non-coding RNA DANCR knockdown-induced suppressive effects on NPC cell migration and invasion[22]. Moreover, inhibition of HIF-1α sensitizes NPC cells to radiotherapy and chemotherapy. Notably, inhibition of hypoxia/radiation-induced upregulation of HIF-1α expression efficiently radio sensitizes NPC cells and xenografts in mice[23]. Reduction of HIF-1α expression reverses EMT and enhances the suppressive effect of 2-Methoxyestradiol on nasopharyngeal carcinoma CNE-2 stem-like cell[24]. Combined with the above researches, both autophagy related proteins and HIF-1α are involved in the malignant progress of NPC, and HIF-1α plays an emerging role in the chemosensitivity of NPC cells. However, it is still unclear whether autophagy related proteins are associated with HIF-1α in affecting the chemosensitivity of NPC cells to cisplatin (DDP), which is the most commonly used chemotherapeutic drug for NPC treatment in clinic[25].

Materials and Methods

Cell Lines

CNE2, 6-10B, SUNE-1, HONE1 and CNE1 cell lines were from the Cell Bank of Type Culture Collection of the Chinese Academy of Sciences (Shanghai, China). These cells were cultured in Dulbecco's Modified Eagle's Medium (DMEM) (Sigma-Aldrich, St. Louis, MO, USA) with 10% fetal bovine serum (Sigma-Aldrich, St. Louis, MO, USA) at 37°C in 5% CO_2 incubator.

Transfection Assay

After grown to 75% confluence, CNE2 or HONE1 cells were transfected with siRNAs or expression plasmids with Lipofectamine 2000 (Invitrogen, Carlsbad, CA, USA) according to the manufacturer's instructions. Then, the corresponding experiments were carried out. The sequences of siRNAs for HIF-1α and ATG4B were shown in Table I.

Quantitative Real-Time PCR (qPCR)

The Total RNA from CNE2 or HONE1 cells was extracted with TRIzol reagent (Comwin Biotechnology, Beijing, China). Next, the first-strand cDNA was synthesized by PrimeScript RT master mix (TaKaRa, Dalian, China). Then, qPCR was carried out with SYBR select master mix (Applied Biosystems, Foster City, CA, USA) according to the manufacturer's instruction, taking β-Actin as a control. The reactions were performed in a 20-μl volume by the following parameters: 95°C for 5 min followed by 40 cycles of 95°C for 15 s and 60°C for 30 s. Subsequently, relative mRNA levels of HIF-1α, ATG3, ATG4B, ATG5, Beclin1, ATG7, ATG10, ATG12 and ATG16L1 were calculated with the $2^{-\Delta\Delta Ct}$ method. The primers were shown in Table II.

Cell Viability Assay

CNE2 or HONE1 cells were transfected with siRNAs or expression plasmids for 24 h. Then, the cell viability was measured by Cell Counting Kit-8 (CCK-8) (Dojindo Laboratories, Kumamoto, Japan). Briefly, the cells were mixed with CCK-

Table I. The sequences of siRNAs.

siRNA	Sequence
siHIF-1α	Forward: 5′-UGGCAGUGUAUUGUUAGCUGGU-3′ Reverse: 5′-ACCAGCUAACAAUACACUGCCA-3′
siATG4B	Forward: 5′-GGUGUGGACAGAUGAUCUUTT-3′ Reverse: 5′-AAGAUCAUCUGUCCACACCTT-3′

Table II. The primer sets for qPCR.

Gene (human)	Primer
HIF-1α	Forward: 5′-GAGGGTGACTGGACTTGTGG-3′ Reverse: 5′-GTAGCAGGACTCCAGGAAGC-3′
ATG3	Forward: 5′-CAGCTGGACACTCAGCTCAA-3′ Reverse: 5′-TTTCCACGTCTTCCAGCTCC-3′
ATG4B	Forward: 5′-GGTGTGGACAGATGATCTTTGC-3′ Reverse: 5′-CCAACTCCCATTTGCGCTATC-3′
ATG5	Forward: 5′-TGGCAGTGTATTGTTAGCTGGT-3′ Reverse: 5′-GGCCAACCGCGAGAAGATGT-3′
Beclin1	Forward: 5′-CTCGCTTCGGCAGCACA-3′ Reverse: 5′-AACGCTTCACGAATTTGCGT-3′
ATG7	Forward: 5′-GGATTCCATGGGGAACTACT-3′ Reverse: 5′-AGTCGTCCTGAGGTTCCAC-3′
ATG10	Forward: 5′-TTCGGAACCATGCGTACA-3′ Reverse: 5′-CCTGGATGGCTTAACCTAGA-3′
ATG12	Forward: 5′-TTCGAAATGGCTAACTAGCA-3′ Reverse: 5′-AATGCTGGCTAGTCTGATC-3′
ATG16L1	Forward: 5′-CGTTGACGTACGATCACCACA-3′ Reverse: 5′-TTCGACGTACATGACAGTAC-3′
β-Actin	Forward: 5′-CGAGGCCCCCCTGAAC-3′ Reverse: 5′-GCCAGAGGCGTACAGGGATA-3′

8 reagent (10 µl per well), and then incubated at 37°C for 1 h. Subsequently, the absorbance of formaldehyde dyes produced by cellular dehydrogenase activity was detected at 450 nm with a microplate reader (Molecular Devices, Sunnyvale, CA, USA). The optical density values represented the cell viability of CNE2 or HONE1 cells.

Analysis of Caspase3 Activity

After corresponding treatment, CNE2 or HONE1 cells were washed in ice-cold phosphate-buffered saline (PBS). Then, the Caspase-3 activity was determined with the colorimetric assay kit (MBL International Corporation, Nagoya, Japan) according to the manufacturer's instruction. First, the proteins were extracted. Second, the cell lysates (20 µl) were added to the buffer containing p-nitroaniline (pNA)-conjugated substrate for Caspase-3 (Ac-DEVD-pNA). Then, the released pNA concentrations were incubated at 37°C and calculated according to the absorbance values at 405 nm. The Caspase-3 activity of the control was set as 100%.

Trypan Blue Exclusion Assay

CNE2 or HONE1 cells were transfected with siRNAs or expression plasmids. Next, the trypan blue exclusion assay was carried out according to the manufacturer's instruction. In brief, the cells were incubated with the trypan blue solution (Beyotime) for 5 min. Then, the cells were photographed using an optical microscope. The cell death rate (%) = number of dead cells/number of total cells (all living and dead cells) × 100%.

Western Blot Analysis

Total protein from CNE2, 6-10B, SUNE-1, HONE1 or CNE1 cells was extracted with RIPA (Beyotime, Shanghai, China). Next, the concentration was detected using the bicinchoninic acid (BCA) Protein Assay Kit (Beyotime). Then, Western blot was performed. In brief, the total proteins (40 µg/well) were separated by 10% sodium dodecyl sulfate polyacrylamide gel electrophoresis (SDS-PAGE), and then transferred to polyvinylidene difluoride (PVDF) membranes (Millipore, Billerica, MA, USA). Then, the PVDF membranes were blocked by 5% non-fat milk for 1 h and incubated with the corresponding antibodies at 4°C for overnight. Subsequently, the blots were washed using Tris-buffered saline and tween-20 (TBST) (Boster, China), and then incubated with the corresponding second antibody at room temperature for 1 h. Ultimately, immunoblots were visualized with the enhanced chemiluminescence (ECL) detection system. The antibodies anti-HIF-1α, anti-ATG4B and anti-cleaved Caspase-3 were from Cell Signaling Technology (CST, Danvers, MA, USA); anti-GAPDH was from Proteintech Group (Chicago, IL, USA).

Plasmid Construction

The expression plasmids pCMV-HIF-1α were from Chongqing Lab Cell Biotechnology Co. Ltd (Chongqing, China). The reporters with different promoter regions of ATG4B gene [pF1 (-2997 to +163), pF2 (-1367 to +163), pF3 (-356 to +163) and pF4 (-179 to +163)] and the pF3 Mut plasmid (-225 GCCCACGTGG -216, the underlined nucleotides were mutated) were purchased from Chongqing Lab Cell Biotechnology Co. Ltd (Chongqing, China).

Luciferase Reporter Assay

CNE2 or HONE1 cells were co-transfected with the Luciferase reporters, pRL-TK plasmid and siRNAs (or expression plasmids). Subsequently, the Luciferase activity was determined with the Dual-Luciferase reporter system (Promega, Madison, WI, USA) according to the manufacturer's instruction. Each reaction was performed three times in triplicate. The ratios of firefly Luciferase activity to *Renilla* Luciferase activity were taken as the results. Data were shown as relative Luciferase activity according to the corresponding control.

Statistical Analysis

Unless otherwise specified, all the results were expressed as mean ± SD. Comparisons for two groups were determined by two-tailed unpaired *t*-test. Comparisons for three or more groups were analyzed using one-way analysis of variance (ANOVA). *p*-value <0.05 was considered statistically significant.

Results

HIF-1α Attenuates the Killing Effect of DDP In NPC Cells

First, the HIF-1α mRNA level was detected in 15 NPC and the corresponding adjacent non-cancerous tissues. The result showed that the mRNA level of HIF-1α was higher in NPC tissues than that in the corresponding adjacent non-cancerous tissues (Figure 1A). Then, the protein level of HIF-1α was determined in five NPC cell lines. As shown in Figure 1B, the HIF-1α protein level was relatively higher in CNE2,

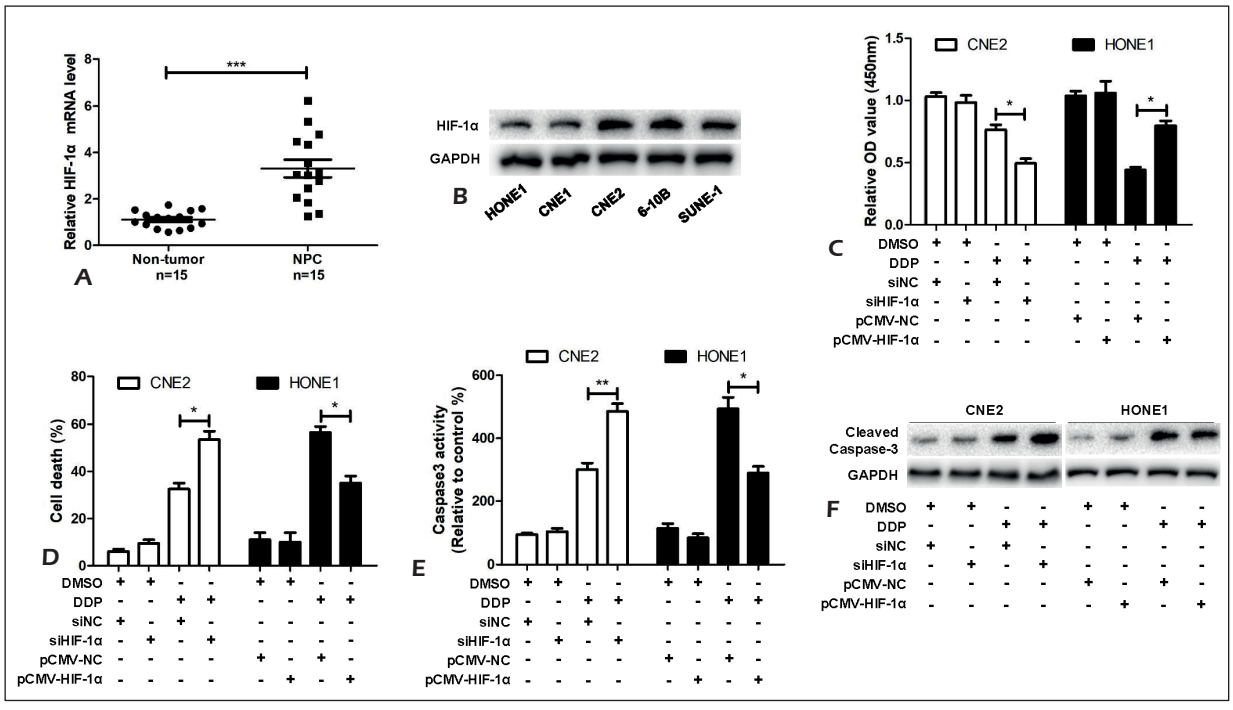

Figure 1. HIF-1α attenuates the killing effect of DDP in NPC cells. **A**, Analysis of HIF-1α mRNA level in 15 NPC and the corresponding adjacent non-cancerous tissues. **B**, Western blot analysis of HIF-1α protein level in 5 NPC cell lines. **C-F**, CNE2 cells were transfected with siHIF-1α or siNC for 24 h, while HONE1 cells were transfected with pCMV-HIF-1α or pCMV-NC for 24 h. Then the cells were treated with DDP (20 μM) or vehicle control DMSO (0.1%) for another 24 h. Later, the optical density values at 450 nm were measured by CCK-8 (**C**), the dead cells were counted after trypan blue exclusion assay (**D**), the Caspase-3 activity was measured to reflect apoptosis (**E**), and the level of cleaved Caspase-3 protein was detected by Western blot (**F**). The OD value at 405 nm in Caspase-3 activity analysis was normalized against that of the control, the control group was defined as 100%. DDP: cisplatin, siHIF-1α: siRNA for HIF-1α, siNC: negative control siRNA, pCMV-HIF-1α: HIF-1α expression vector. **p*<0.05, ***p*<0.01, ****p*<0.001.

6-10B and SUNE-1 cell lines, and relatively lower in HONE1 and CNE1 cell lines. Then, the CNE2 cell line (with higher HIF-1α expression) and HONE1 cell line (with lower HIF-1α expression) were selected for the following experiments. Figures 1C-F showed that silence of HIF-1α in CNE2 cells enhanced the DDP-induced decrease of cell viability (Figure 1C), increase of cell death (Figure 1D) and increase of Caspase-3 activity (Figure 1E) and cleavage (Figure 1F). While overexpression of HIF-1α in HONE1 cells attenuated the DDP-triggered decrease of cell viability (Figure 1C), increase of cell death (Figure 1D) and increase of Caspase-3 activity (Figure 1E) and cleavage (Figure 1F). These data indicated that HIF-1α attenuates the killing effect of DDP in NPC cells.

HIF-1α Enhances the DDP-Induced Protective Autophagy

To investigate whether HIF-1α-mediated low sensitivity of NPC cells to DDP was associated with autophagy, the following experiments were performed. As shown in Figures 2A-D, the autophagy inhibitor chloroquine significantly enhanced the DDP-induced decrease of cell viability (Figure 2A), increase of cell death (Figure 2B) and increase of Caspase-3 activity (Figure 2C) and cleavage (Figure 2D) in CNE2 cells. These results showed that autophagy was responsible for the low sensitivity of NPC cells to DDP. Moreover, silence of HIF-1α in CNE2 cells significantly attenuated the DDP-induced decline of SQSTM1 protein level (Figure 2E). While overexpression of HIF-1α in HONE1 cells remarkably enhanced the EPI-triggered decrease of SQSTM1 protein level (Figure 2E). Additionally, suppression of autophagy with chloroquine did not further strengthen the decrease of cell viability (Figure 2F), the increase of cell death (Figure 2G) and the increase of Caspase-3 activity (Figure 2H) and cleavage (Figure 2I) upon co-treatment with DDP and HIF-1α siRNA. These results indicated that HIF-1α attenuates the sensitivity of NPC cells to DDP by enhancing the DDP-induced protective autophagy.

HIF-1α Strengthens the DDP-Triggered Protective Autophagy Via Upregulating ATG4B

To explore the mechanism by which HIF-1α enhanced the DDP-induced protective autophagy in NPC cells, the mRNA levels of eight autophagy related genes were detected. As shown in Figures 3A and 3B, silence of HIF-1α in CNE2 cells decreased the mRNA level of ATG4B (Figure 3A), while overexpression of HIF-1α in HONE1 cells increased the mRNA level of ATG4B (Figure 3B). Figure 3C showed that the protein level of ATG4B was downregulated by silence of HIF-1α in CNE2 cells and upregulated by overexpression of HIF-1α in HONE1 cells. Furthermore, silence of ATG4B in HONE1 cells significantly alleviated the HIF-1α-induced decrease of SQSTM1 protein upon DDP treatment (Figure 3D). Meanwhile, silence of ATG4B in HONE1 cells remarkably attenuated the HIF-1α-induced increase of cell viability (Figure 3E) and decrease of Caspase-3 cleavage upon DDP treatment (Figure 3F). In brief, the above results indicated that HIF-1α elevates ATG4B expression, which enhances the DDP-induced protective autophagy in NPC cells.

HIF-1α Increased ATG4B Expression by Activating Its Gene Promoter Region

To investigate the mechanism by which HIF-1α elevated ATG4B mRNA, actinomycin D (a transcription inhibitor) assays were firstly performed. As shown in Figures 4A and 4B, silence of HIF-1α in CNE2 cells (Figure 4A) or overexpression of HIF-1α in HONE1 cells (Figure 4B) did not influence the degradation speed of ATG4B mRNA, indicating that HIF-1α did not affect ATG4B mRNA stability. Next, four Luciferase reporter plasmids with different ATG4B gene promoter regions were constructed, which were separately named as pF1 (-2997 to +163), pF2 (-1367 to +163), pF3 (-356 to +163) and pF4 (-179 to +163). Then, the Luciferase reporter assays were performed, showing that silence of HIF-1α in CNE2 cells significantly reduced the activity of pF1, pF2 and pF3 rather than pF4 (Figure 4C), while overexpression of HIF-1α in HONE1 cells markedly increased the activity of pF1, pF2 and pF3 rather than pF4 (Figure 4D). These results revealed that a HIF-1α binding site may be within the sequence (-356 to -179) of ATG4B promoter region. Based on online prediction, the binding site in the sequence (-356 to -179) should be (-225 to -216). Moreover, silence or overexpression of HIF-1α did not influence the activity of pF3 Mut (containing mutations in the sequence -225 to -216) (Figures 4E and 4F). These data indicated that HIF-1α increased ATG4B expression by activating its gene promoter region, and the potential binding site (-225 to -216) was required for HIF-1α-induced increase of ATG4B gene promoter activity.

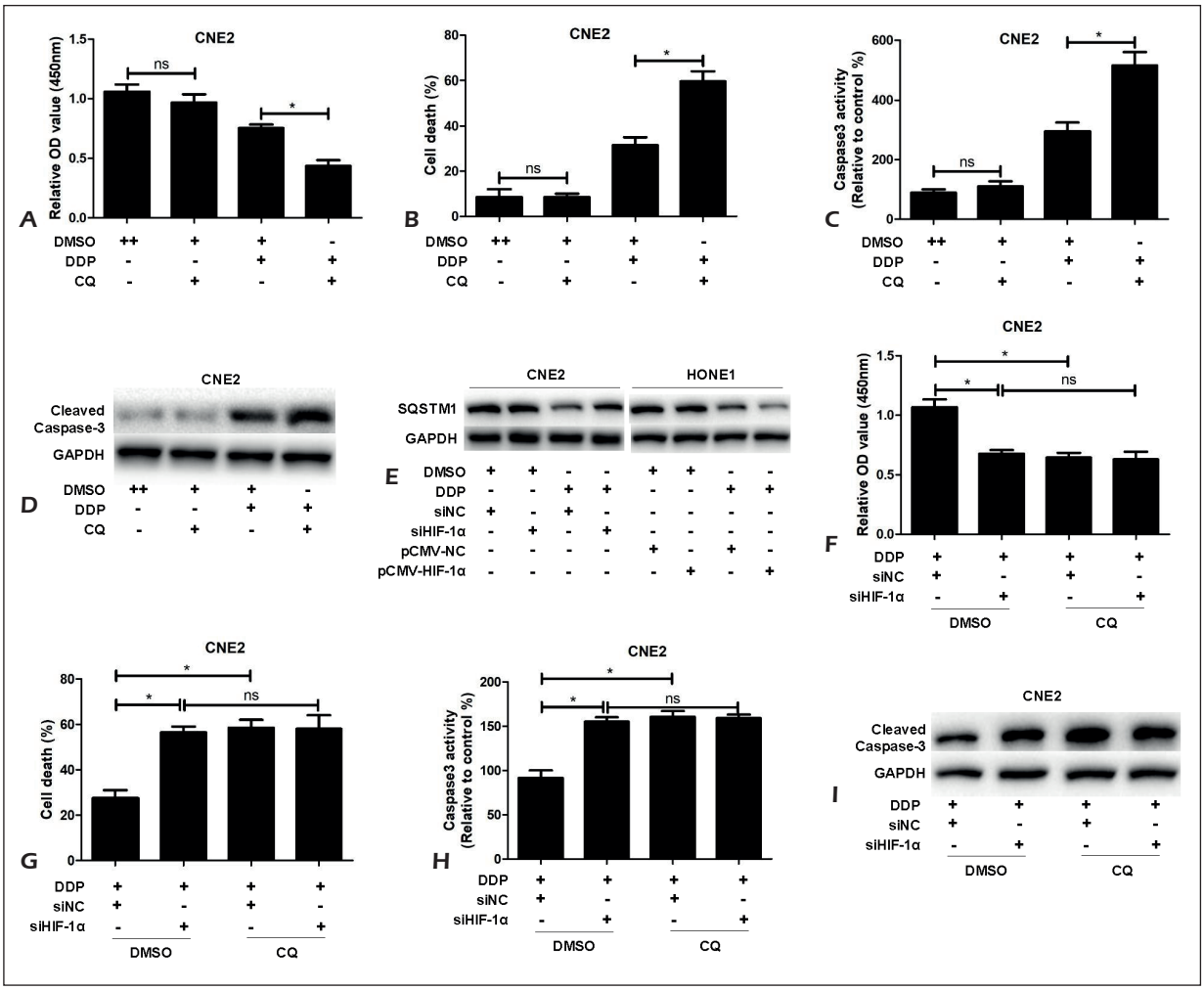

Figure 2. HIF-1α enhances the DDP-induced protective autophagy. **A**-**D**, CNE2 cells were treated with CQ (20 mM) or vehicle control DMSO (0.1%) in the presence or absence of DDP (20 μM) for 24 h. Then, the optical density values at 450 nm were measured by CCK-8 (**A**), the dead cells were counted after trypan blue exclusion assay (**B**), the Caspase-3 activity was measured to reflect apoptosis (**C**), and the level of cleaved Caspase-3 protein was detected by Western blot (**D**). **E**, CNE2 cells were transfected with siHIF-1α (or siNC) for 24 h, while HONE1 cells were transfected with pCMV-HIF-1α (or pCMV-NC) for 24 h. Then, the cells were treated with DDP (20 μM) or DMSO (0.1%) for another 24 h. Subsequently, the levels of SQSTM1 were examined by Western blot. **F**-**I**, After transfected with siHIF-1α or siNC for 24 h, the CNE2 cells were treated with CQ (20 mM) or DMSO (0.1%) in the presence of DDP (20 μM) for another 24 h. Then, the cell viability was determined by CCK8 assay. Then, the optical density values at 450 nm were measured by CCK-8 (**F**), the dead cells were counted after trypan blue exclusion assay (**G**), the Caspase-3 activity was measured to reflect apoptosis (**H**), and the level of cleaved Caspase-3 protein was detected by Western blot (**I**). The OD value at 405 nm in Caspase-3 activity analysis was normalized against that of the control, the control group was defined as 100%. DDP: cisplatin, CQ: chloroquine, siHIF-1α: siRNA for HIF-1α, siNC: negative control siRNA, pCMV-HIF-1α: HIF-1α expression vector. ns: no significance, *p<0.05.

Discussion

DDP is a non-specific drug of cell cycle, which is cytotoxic[26]. Since the proliferation and synthesis of cancer cells are faster than that of normal cells, cancer cells are more sensitive to the cytotoxic effect of DDP, which can inhibit the DNA replication process of cancer cells, damage the structure of their cell membrane, and has a strong broad-spectrum anti-cancer effect[27,28]. DDP is the first-line therapeutic administration in NPC patients[29]. However, in the treatment of NPC, low chemosensitivity has been a main barrier, leading to bad treatment outcome[30]. In this study, we found that silence of HIF-1α decreased the ATG4B expression, and in turn enhanced the chemosensitivity of NPC cells to DDP, providing a novel target for improving the sensitivity of NPC cells to DPP.

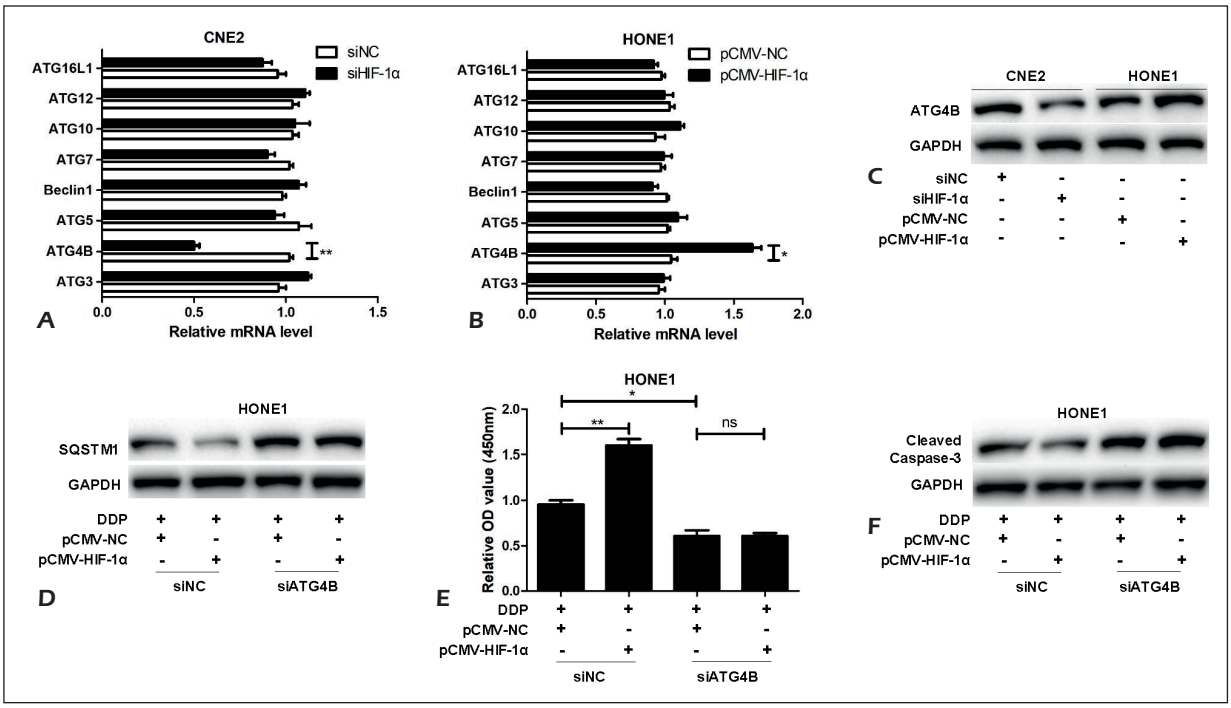

Figure 3. HIF-1α strengthens the DDP-triggered protective autophagy via upregulating ATG4B. **A**-**C**, CNE2 cells (**A**, **C**) were transfected with siHIF-1α or siNC for 24 h, while HONE1 cells (**B**, **C**) were transfected with pCMV-HIF-1α or pCMV-NC for 24 h. Then, the mRNA levels of 8 autophagy related genes were detected by qPCR (**A**, **B**) and the protein level of ATG4B was assayed by Western blot (**C**). **D**-**F**, after transfected with pCMV-HIF-1α or pCMV-NC in the presence or absence of siATG4B for 24 h, the HONE1 cells were treated with DDP (20 μM) for another 24 h. Then, the level of SQSTM1 was determined by Western blot, the cell viability was determined by CCK8 assay (**E**), and the level of cleaved Caspase-3 protein was detected by Western blot (**F**). DDP: cisplatin, siATG4B: siRNA for ATG4B, siHIF-1α: siRNA for HIF-1α, siNC: negative control siRNA, pCMV-HIF-1α: HIF-1α expression vector. ns: no significance, *p<0.05, **p<0.01.

ATG4B is a key protein regulating the formation of autophagosomes in mammalian cells[31]. In the process of autophagosomes formation, the cytoplasm LC3 is cleaved to LC3-I at its C-terminal arginine residue, and then LC3-I combined with phosphatidylethanolamine and converted to membrane-bound LC3-II[32]. ATG4B plays an important role in the processes of cleaving cytoplasmic LC3 and deconjugating LC3-II[32]. Some evidence[33,34] has shown that ATG4B has an important impact on autophagy and further leads to chemoresistance in various tumor cells. For example, upregulation of ATG4B has been reported to induce autophagy, thereby reducing the sensitivity of prostate and lung cancer cells to chemotherapy[35,36]. In addition, silence of ATG4B suppresses autophagy, which subsequently inhibits the survival of chronic myeloid leukemia stem/progenitor cells, and increases the sensitivity to imatinib mesylate[37]. In this study, we for the first time demonstrated that ATG4B, which could be upregulated by HIF-1α, enhanced the DDP-induced protective autophagy in NPC cells, revealing that ATG4B may be a novel target for the treatment of NPC in clinic.

Autophagy is a lysosomal mediated process of intracellular self-catabolism, which is characterized by the formation of double membrane vesicles, called autophagosomes[38]. Autophagosomes phagocytized a large number of cytoplasm, damaged proteins and organelles, and then fused with lysosomes to form autolysosomes[39]. The contents of autolysosomes are digested by lysosomal hydrolase, then circulated and decomposed[40,41]. Increasing evidence confirmed the importance of autophagy in determining the response of tumor cells to anticancer therapy[42]. It has been reported that autophagy is closely associated with NPC[43,44]. Xie et al[43] have reported that autophagy can be triggered by silence of cyclinB1 via AMPK-ULK1-dependent signal pathway in NPC cells. Tan et al[44] have reported that autophagy is enhanced by inhibiting the extracellular regulated protein kinases (ERK) pathway, and that autophagy plays a protective role against apoptosis in the NPC CNE-2 cell line. In this study, we re-

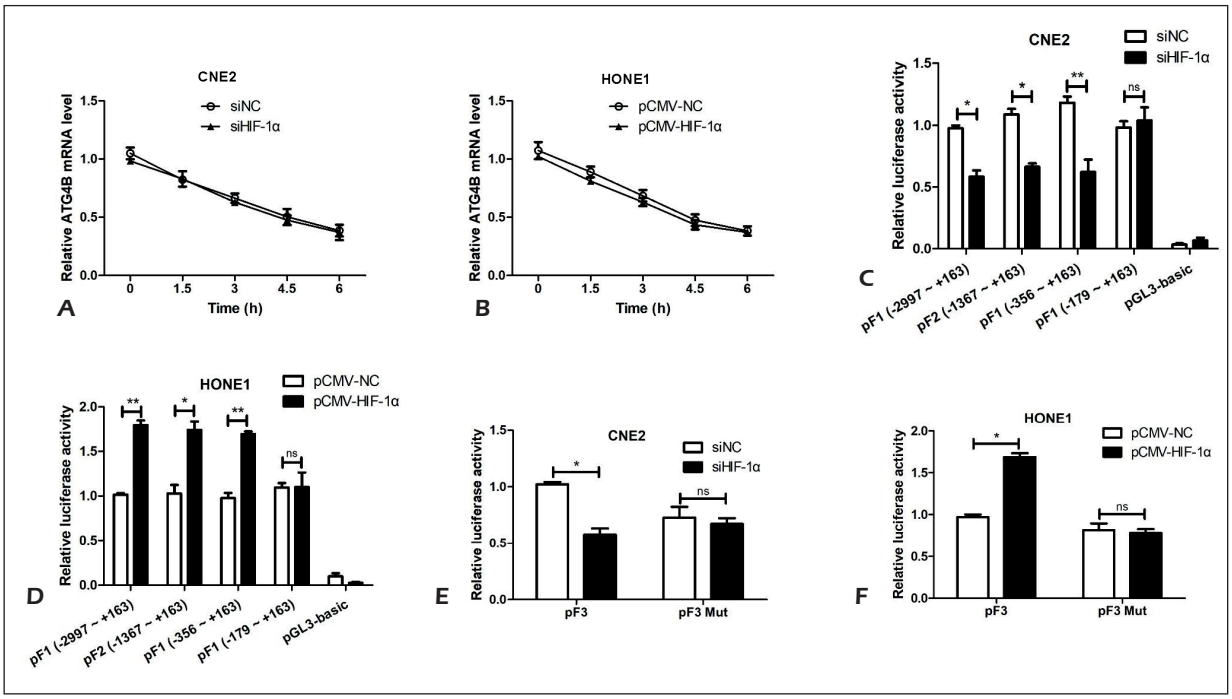

Figure 4. HIF-1α increased ATG4B expression by activating its gene promoter region. ***A*-*B***, CNE2 cells (***A***) were transfected with siHIF-1α (or siNC) and HONE1 cells (***B***) were transfected with pCMV-HIF-1α (or pCMV-NC) for 24 h, followed by the treatment with Act D (5 mg/ml) for the indicated time. Then, the level of ATG4B mRNA was detected by qPCR. ***C*-*F***, After co-transfected with the Luciferase reporters (or pF3 Mut) and pRL-TK in the presence of siHIF-1α (or siNC) (for CNE2 cells) (***C*-*E***) or pCMV-HIF-1α (or pCMV-NC) (for HONE1 cells) (***D*-*F***) for 24 h. The Luciferase activity was measured with the Dual-Luciferase reporter system. The firefly Luciferase activity was normalized against the Renilla Luciferase activity. Act D: actinomycin D, siHIF-1α: siRNA for HIF-1α, siNC: negative control siRNA, pCMV-HIF-1α: HIF-1α expression vector, pF3 Mut: pF3 mutant. ns: no significance, *$p<0.05$, **$p<0.01$.

vealed that inhibiting autophagy by chloroquine or ATG4B siRNA enhanced the killing effect of DDP to NPC cells. Therefore, targeting autophagy to improve the chemosensitivity of NPC cells may have great significance and broad clinical application prospects; however, more studies are needed.

Conclusions

In summary, for the first time we demonstrated that HIF-1α increases ATG4B expression in NPC cells by activating its gene promoter region, which enhanced the DDP-induced protective autophagy and subsequently promoted NPC cell survival upon DDP treatment. Moreover, inhibition of the "HIF-1α/ATG4B/protective autophagy" pathway increased the sensitivity of NPC cells to DDP, suggesting that ATG4B, upregulated by HIF-1α, may serve as a novel target of chemotherapy sensitization strategy for NPC in clinic.

Conflict of Interests

The authors declare that they have no conflict of interests.

References

1) Chen YP, Chan ATC, Le QT, Blanchard P, Sun Y, Ma J. Nasopharyngeal carcinoma. Lancet 2019; 394: 64-80.
2) Cai J, Chen S, Yi M, Tan Y, Peng Q, Ban Y, Yang J, Li X, Zeng Z, Xiong W, McCarthy J B, Li G, Li X, Xiang B. DeltaNp63alpha is a super enhancer-enriched master factor controlling the basal-to-luminal differentiation transcriptional program and gene regulatory networks in nasopharyngeal carcinoma. Carcinogenesis. 2019 Dec 12. pii: bgz203. doi: 10.1093/carcin/bgz203. [Epub ahead of print].
3) Lee AW, Ma BB, Ng WT, Chan AT. Management of nasopharyngeal carcinoma: current practice and future perspective. J Clin Oncol 2015; 33: 3356-3364.
4) Bruce JP, Yip K, Bratman SV, Ito E, Liu FF. Nasopharyngeal cancer: molecular landscape. J Clin Oncol 2015; 33: 3346-3355.

5) Zhao Y, Liu H, Liu Z, Ding Y, Ledoux SP, Wilson G L, Voellmy R, Lin Y, Lin W, Nahta R, Liu B, Fodstad O, Chen J, Wu Y, Price JE, Tan M. Overcoming trastuzumab resistance in breast cancer by targeting dysregulated glucose metabolism. Cancer Res 2011; 71: 4585-4597.
6) Peng S, Wang Y, Peng H, Chen D, Shen S, Peng B, Chen M, Lencioni R, Kuang M. Autocrine vascular endothelial growth factor signaling promotes cell proliferation and modulates sorafenib treatment efficacy in hepatocellular carcinoma. Hepatology 2014; 60: 1264-1277.
7) Rudalska R, Dauch D, Longerich T, McJunkin K, Wuestefeld T, Kang TW, Hohmeyer A, Pesic M, Leibold J, von Thun A, Schirmacher P, Zuber J, Weiss KH, Powers S, Malek NP, Eilers M, Sipos B, Lowe SW, Geffers R, Laufer S, Zender L. *In vivo* RNAi screening identifies a mechanism of sorafenib resistance in liver cancer. Nat Med 2014; 20: 1138-1146.
8) Pohl C, Dikic I. Cellular quality control by the ubiquitin-proteasome system and autophagy. Science 2019; 366: 818-822.
9) Kirkin V, Rogov VV. A diversity of selective autophagy receptors determines the specificity of the autophagy pathway. Mol Cell 2019; 76: 268-285.
10) Ruan S, Xie R, Qin L, Yu M, Xiao W, Hu C, Yu W, Qian Z, Ouyang L, He Q, Gao H. Aggregable nanoparticles-enabled chemotherapy and autophagy inhibition combined with anti-PD-L1 antibody for improved glioma treatment. Nano Lett 2019; 19: 8318-8332.
11) Vehlow A, Cordes N. DDR1 (discoidin domain receptor tyrosine kinase 1) drives glioblastoma therapy resistance by modulating autophagy. Autophagy 2019; 15: 1487-1488.
12) Zhu JF, Huang W, Yi HM, Xiao T, Li JY, Feng J, Yi H, Lu SS, Li XH, Lu RH, He QY, Xiao ZQ. Annexin A1-suppressed autophagy promotes nasopharyngeal carcinoma cell invasion and metastasis by PI3K/AKT signaling activation. Cell Death Dis 2018; 9: 1154.
13) Yang Q, Zhang MX, Zou X, Liu YP, You R, Yu T, Jiang R, Zhang YN, Cao JY, Hong MH, Liu Q, Guo L, Kang TB, Zhu XF, Chen MY. A prognostic bio-model based on SQSTM1 and N-stage identifies nasopharyngeal carcinoma patients at high risk of metastasis for additional induction chemotherapy. Clin Cancer Res 2018; 24: 648-658.
14) Lin YT, Wang HC, Chuang HC, Hsu YC, Yang MY, Chien CY. Pre-treatment with angiotensin-(1-7) inhibits tumor growth via autophagy by downregulating PI3K/Akt/mTOR signaling in human nasopharyngeal carcinoma xenografts. J Mol Med (Berl) 2018; 96: 1407-1418.
15) Makowska A, Eble M, Prescher K, Hoss M, Kontny U. Chloroquine sensitizes nasopharyngeal carcinoma cells but not nasoepithelial cells to irradiation by blocking autophagy. PLoS One 2016; 11: e0166766.
16) Knight M, Stanley S. HIF-1alpha as a central mediator of cellular resistance to intracellular pathogens. Curr Opin Immunol 2019; 60: 111-116.
17) Warbrick I, Rabkin SW. Hypoxia-inducible factor 1-alpha (HIF-1alpha) as a factor mediating the relationship between obesity and heart failure with preserved ejection fraction. Obes Rev 2019; 20: 701-712.
18) Hatfield S, Veszeleiova K, Steingold J, Sethuraman J, Sitkovsky M. Mechanistic justifications of systemic therapeutic oxygenation of tumors to weaken the hypoxia inducible factor 1alpha-mediated immunosuppression. Adv Exp Med Biol 2019; 1136: 113-121.
19) Aga M, Bentz GL, Raffa S, Torrisi MR, Kondo S, Wakisaka N, Yoshizaki T, Pagano JS, Shackelford J. Exosomal HIF1alpha supports invasive potential of nasopharyngeal carcinoma-associated LMP1-positive exosomes. Oncogene 2014; 33: 4613-4622.
20) Hayashi Y, Yokota A, Harada H, Huang G. Hypoxia/pseudohypoxia-mediated activation of hypoxia-inducible factor-1alpha in cancer. Cancer Sci 2019; 110: 1510-1517.
21) Shan Y, You B, Shi S, Shi W, Zhang Z, Zhang Q, Gu M, Chen J, Bao L, Liu D, You Y. Hypoxia-induced matrix metalloproteinase-13 expression in exosomes from nasopharyngeal carcinoma enhances metastases. Cell Death Dis 2018; 9: 382.
22) Wen X, Liu X, Mao YP, Yang XJ, Wang YQ, Zhang PP, Lei Y, Hong XH, He QM, Ma J, Liu N, Li YQ. Long non-coding RNA DANCR stabilizes HIF-1alpha and promotes metastasis by interacting with NF90/NF45 complex in nasopharyngeal carcinoma. Theranostics 2018; 8: 5676-5689.
23) Zhang C, Yang X, Zhang Q, Yang B, Xu L, Qin Q, Zhu H, Liu J, Cai J, Tao G, Ma J, Ge X, Zhang S, Cheng H, Sun X. Berberine radiosensitizes human nasopharyngeal carcinoma by suppressing hypoxia-inducible factor-1alpha expression. Acta Otolaryngol 2014; 134: 185-192.
24) Wu SL, Li YJ, Liao K, Shi L, Zhang N, Liu S, Hu YY, Li SL, Wang Y. 2-Methoxyestradiol inhibits the proliferation and migration and reduces the radioresistance of nasopharyngeal carcinoma CNE-2 stem cells via NF-kappaB/HIF-1 signaling pathway inactivation and EMT reversal. Oncol Rep 2017; 37: 793-802.
25) Zhang Y, Chen L, Hu GQ, Zhang N, Zhu XD, Yang KY, Jin F, Shi M, Chen YP, Hu WH, Cheng ZB, Wang SY, Tian Y, Wang XC, Sun Y, Li JG, Li WF, Li YH, Tang LL, Mao YP, Zhou GQ, Sun R, Liu X, Guo R, Long GX, Liang SQ, Li L, Huang J, Long JH, Zang J, Liu QD, Zou L, Su QF, Zheng BM, Xiao Y, Guo Y, Han F, Mo HY, Lv JW, Du XJ, Xu C, Liu N, Li YQ, Chua MLK, Xie FY, Sun Y, Ma J. Gemcitabine and cisplatin induction chemotherapy in nasopharyngeal carcinoma. N Engl J Med 2019; 381: 1124-1135.
26) Fang W, Yang Y, Ma Y, Hong S, Lin L, He X, Xiong J, Li P, Zhao H, Huang Y, Zhang Y, Chen L, Zhou N, Zhao Y, Hou X, Yang Q, Zhang L. Camrelizumab (SHR-1210) alone or in combination with gemcitabine plus cisplatin for nasopharyngeal carcinoma: results from two single-arm, phase 1 trials. Lancet Oncol 2018; 19: 1338-1350.
27) Zhang L, Huang Y, Hong S, Yang Y, Yu G, Jia J, Peng P, Wu X, Lin Q, Xi X, Peng J, Xu M, Chen D, Lu X, Wang R, Cao X, Chen X, Lin Z, Xiong J, Lin Q, Xie C, Li Z, Pan J, Li J, Wu S, Lian Y, Yang Q, Zhao C. Gemcitabine plus cisplatin versus fluorouracil plus cisplatin in recurrent or metastatic nasopharyngeal carcinoma: a multicentre, randomised, open-label, phase 3 trial. Lancet 2016; 388: 1883-1892.

28) Hui EP, Ma BB, Leung SF, King AD, Mo F, Kam MK, Yu BK, Chiu SK, Kwan WH, Ho R, Chan I, Ahuja AT, Zee BC, Chan AT. Randomized phase II trial of concurrent cisplatin-radiotherapy with or without neoadjuvant docetaxel and cisplatin in advanced nasopharyngeal carcinoma. J Clin Oncol 2009; 27: 242-249.
29) Chan AT, Leung SF, Ngan RK, Teo PM, Lau WH, Kwan WH, Hui EP, Yiu HY, Yeo W, Cheung FY, Yu KH, Chiu KW, Chan DT, Mok TS, Yau S, Yuen KT, Mo FK, Lai MM, Ma BB, Kam MK, Leung TW, Johnson PJ, Choi PH, Zee BC. Overall survival after concurrent cisplatin-radiotherapy compared with radiotherapy alone in locoregionally advanced nasopharyngeal carcinoma. J Natl Cancer Inst 2005; 97: 536-539.
30) Li S, Zhang X, Zhang R, Liang Z, Liao W, Du Z, Gao C, Liu F, Fan Y, Hong H. Hippo pathway contributes to cisplatin resistant-induced EMT in nasopharyngeal carcinoma cells. Cell Cycle 2017; 16: 1601-1610.
31) Shin JH, Park SJ, Jo DS, Park NY, Kim JB, Bae JE, Jo YK, Hwang JJ, Lee JA, Jo DG, Kim JC, Jung YK, Koh JY, Cho DH. Down-regulated TMED10 in Alzheimer disease induces autophagy via ATG4B activation. Autophagy 2019; 15: 1495-1505.
32) Agrotis A, Pengo N, Burden JJ, Ketteler R. Redundancy of human ATG4 protease isoforms in autophagy and LC3/GABARAP processing revealed in cells. Autophagy 2019; 15: 976-997.
33) Fu Y, Hong L, Xu J, Zhong G, Gu Q, Gu Q, Guan Y, Zheng X, Dai Q, Luo X, Liu C, Huang Z, Yin XM, Liu P, Li M. Discovery of a small molecule targeting autophagy via ATG4B inhibition and cell death of colorectal cancer cells in vitro and in vivo. Autophagy 2019; 15: 295-311.
34) Huang T, Kim CK, Alvarez AA, Pangeni RP, Wan X, Song X, Shi T, Yang Y, Sastry N, Horbinski CM, Lu S, Stupp R, Kessler JA, Nishikawa R, Nakano I, Sulman EP, Lu X, James CD, Yin XM, Hu B, Cheng SY. MST4 phosphorylation of atg4b regulates autophagic activity, tumorigenicity, and radioresistance in glioblastoma. Cancer Cell 2017; 32: 840-855.e8.
35) Liao H, Xiao Y, Hu Y, Xiao Y, Yin Z, Liu L, Kang X, Chen Y. Methylation-induced silencing of miR-34a enhances chemoresistance by directly upregulating ATG4B-induced autophagy through AMPK/mTOR pathway in prostate cancer. Oncol Rep 2016; 35: 64-72.
36) Wu S, Su J, Qian H, Guo T. SLC27A4 regulate ATG4B activity and control reactions to chemotherapeutics-induced autophagy in human lung cancer cells. Tumour Biol 2016; 37: 6943-6952.
37) Rothe K, Lin H, Lin KB, Leung A, Wang HM, Malekesmaeili M, Brinkman RR, Forrest DL, Gorski SM, Jiang X. The core autophagy protein ATG4B is a potential biomarker and therapeutic target in CML stem/progenitor cells. Blood 2014; 123: 3622-3634.
38) Nakashima A, Cheng S B, Ikawa M, Yoshimori T, Huber W J, Menon R, Huang Z, Fierce J, Padbury J F, Sadovsky Y, Saito S, Sharma S. Evidence for lysosomal biogenesis proteome defect and impaired autophagy in preeclampsia. Autophagy. 2019 Dec 26:1-15. doi: 10.1080/15548627.2019.1707494. [Epub ahead of print].
39) Gassen N C, Niemeyer D, Muth D, Corman V M, Martinelli S, Gassen A, Hafner K, Papies J, Mosbauer K, Zellner A, Zannas A S, Herrmann A, Holsboer F, Brack-Werner R, Boshart M, Muller-Myhsok B, Drosten C, Muller M A, Rein T. SKP2 attenuates autophagy through Beclin1-ubiquitination and its inhibition reduces MERS-Coronavirus infection. Nat Commun 2019; 10: 5770.
40) Tang F, Gao R, Jeevan-Raj B, Wyss CB, Kalathur RKR, Piscuoglio S, Ng CKY, Hindupur SK, Nuciforo S, Dazert E, Bock T, Song S, Buechel D, Morini MF, Hergovich A, Matthias P, Lim DS, Terracciano LM, Heim MH, Hall MN, Christofori G. LATS1 but not LATS2 represses autophagy by a kinase-independent scaffold function. Nat Commun 2019; 10: 5755.
41) Zhang X, Wu D, Wang C, Luo Y, Ding X, Yang X, Silva F, Arenas S, Weaver JM, Mandell M, Deretic V, Liu M. Sustained activation of autophagy suppresses adipocyte maturation via a lipolysis-dependent mechanism. Autophagy 2019 Dec 18:1-15. doi: 10.1080/15548627.2019.1703355. [Epub ahead of print].
42) Zhang Y, Zhang L, Gao J, Wen L. Pro-Death or pro-survival: contrasting paradigms on nanomaterial-induced autophagy and exploitations for cancer therapy. Acc Chem Res 2019; 52: 3164-3176.
43) Xie X, Lin W, Zheng W, Chen T, Yang H, Sun L, Huang F, Wang Z, Lin H, Chen L, Liu J, Yang L. Downregulation of G2/mitotic-specific cyclinB1 triggers autophagy via AMPK-ULK1-dependent signal pathway in nasopharyngeal carcinoma cells. Cell Death Dis 2019; 10: 94.
44) Tan GX, Wang XN, Tang YY, Cen WJ, Li ZH, Wang GC, Jiang JW, Wang XC. PP-22 promotes autophagy and apoptosis in the nasopharyngeal carcinoma cell line CNE-2 by inducing endoplasmic reticulum stress, downregulating STAT3 signaling, and modulating the MAPK pathway. J Cell Physiol 2019; 234: 2618-2630.